Measuring swash zone hydrodynamics and morphodynamic change – a high-resolution laboratory system using digital video

Authors: Foote, Matthew, Horn, Diane, and Li, Ling

Source: Journal of Coastal Research, 36(sp1) : 300-316

Published By: Coastal Education and Research Foundation

URL: https://doi.org/10.2112/1551-5036-36.sp1.300

Journal of Coastal Research	SI 36	300-316	(ICS 2002 Proceedings)	Northern Ireland	ISSN 0749-0208

Measuring swash zone hydrodynamics and morphodynamic change – a high-resolution laboratory system using digital video

Matthew Foote †, Diane Horn †* and Ling Li ‡

†School of Geography
Birkbeck College, University of London
7-15 Gresse Street
London W1P 2LL
d.horn@bbk.ac.uk
* corresponding author

‡School of Civil and Environmental Engineering
Contaminated Land Assessment and Remediation
Research Centre
The University of Edinburgh
Edinburgh EH9 3JN

ABSTRACT

An important area of uncertainty in swash sediment transport modelling is the impact that swash lens hydrodynamics, including flow velocity and local swash depth, may have on the direction and magnitude of net sediment transport over time, and hence the morphological evolution of the beachface. Swash, as manifested in the instantaneous shape of the lens, may be categorised as uprush, 'flow reversal'or backwash, each phase having a characteristic hydrodynamic regime. However, the exact character of each phase, including the appearance of hydraulic jumps or retrogressive bores as well as the depth and flow velocity of the lens, are determined by a complex interaction between antecedent beachface conditions, beach groundwater dynamics and initial hydrodynamic inputs. Measurement of swash processes using conventional fixed instruments does not provide the temporal or spatial resolution necessary to adequately quantify or even identify the relationship between these factors.

Video imaging of the two-dimensional, cross-shore water surface and beachface provides a means of acquiring high-resolution data of the water surface and beachface morphology. Previous experiments have used analogue camcorder technology and associated image processing and geographical information systems (GIS) technology to capture water surface information. Due to image degradation from the analogue interleaving process, manual digitisation of the water surface was found to be the most practical data capture technique.

The aim of this research was to capture two-dimensional images of the swash lens in a laboratory flume using a digital video camera recording direct to PC hard drive and to compare to water depth data captured using a capacitance probe. Digital video capture has a number of potential advantages over conventional analogue video, including:

- the removal of the post-capture analogue to digital conversion stage (frame-grabbing) and
- improved geometric and radiometric image quality, both resulting in higher spatial resolution.

The results of this comparison suggest that the data captured by the digital video system are comparable in resolution to that collected by the wave gauge. Suggestions as to the future use of IEEE1394 video technology for swash measurement and possible improvements to the data capture mechanism are made.

INTRODUCTION

Swash zone processes and measurements

Interest in the geomorphology of the swash zone has increased over the past few years as the importance of swash processes in determining net sediment transport rates and hence accretion or deposition has become clearer. Most recently, computational process-based swash models have made significant advances in the transition from lumped conceptualisation to quantitative description of the hydrodynamic and morphodynamic regimes operating in the swash zone. Research such as that undertaken by HUGHES (1992, 1995), HUGHES *et al*. (1997), MASSELINK and HUGHES (1998), PULEO *et al*. (2000) and MASSELINK and LI (2001) has applied numerical models and empirical observations of the swash process to sediment transport problems.

Much of this research has concentrated on linking well-known sediment transport models such as the Bagnold-type bedload (for example HUGHES *et al*., 2000; PULEO *et al*., 2000; MASSELINK and LI, 2001) with the non-linear shallow water (NLSW) model (HUGHES, 1995). Such research attempts to predict sediment yield at the individual swash event scale and therefore the rate and direction of morphodynamic change.

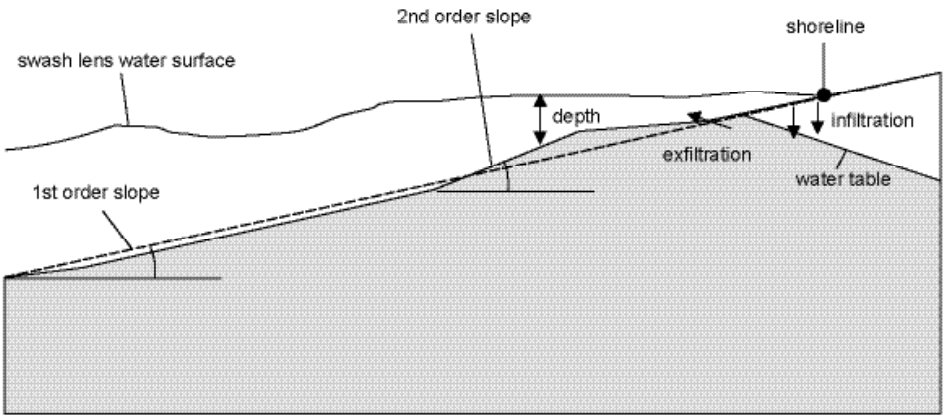

Figure 1. Cross-shore swash zone definition.

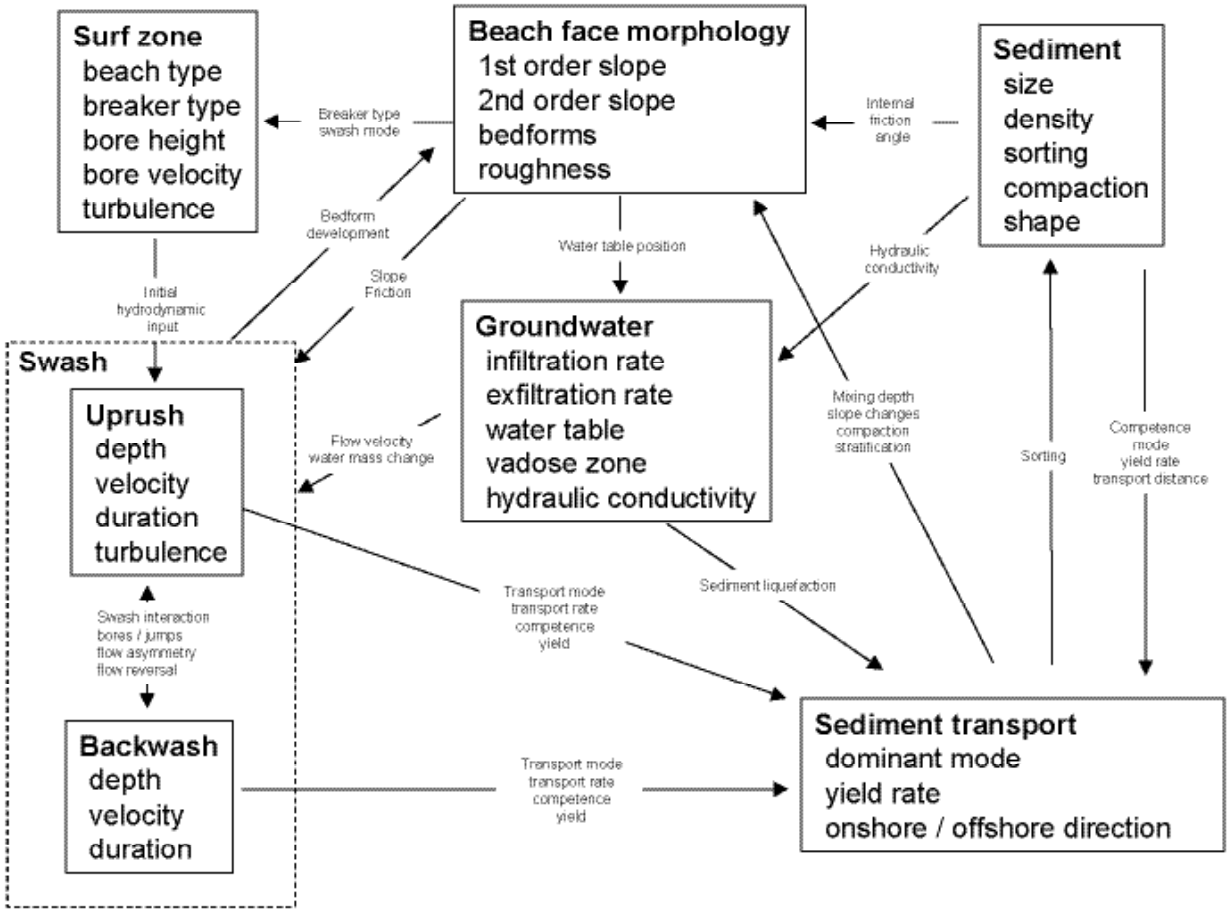

Figure 2. Lumped conceptual model of the geomorphological swash system. Arrows indicate major direct controls on each sub-system. To aid clarity, the reader should first direct their attention to the morphology subsystem.

Software such as BeachWin (LI *et al*., in press), which couples together hydrodynamic inputs with morphodynamic and groundwater effects, has recently provided a means of replicating the complete two-dimensional (cross-shore) geomorphological system operating within the swash zone from a series of basic inputs.

Of particular interest is the precise nature of flow asymmetry between the uprush and backwash phases, as manifested by differences in the instantaneous cross-shore depth of the swash lens, the velocity of the swash flow and the duration of the flow (Figure 1). Based on LI *et al*.'s (in press) model, MASSELINK and LI (2001) examined the mechanism whereby swash asymmetry may become the primary determinant of net sediment transport at the individual swash event scale, with swash infiltration on the uprush phase reducing the amount of water available for backwash (seawards) transport of sediment initially carried landward. Frictional retardation will also influence the nature of the flow asymmetry between the uprush and backwash phases. Other factors, which may also influence flow asymmetry, are the formation of hydraulic jumps and bores within the backwash phase of the swash. The model assumes an equilibrium state will eventually be reached which is determined by the sediment size, swash depth and velocity and infiltration rate (as determined by the hydraulic conductivity of the beach matrix). The LI *et al*. model provides estimates of beach face geometry change (due to net accretion / erosion) at the swash event scale as well as the water surface geometry of the swash event in both uprush and backwash phases.

The complexity of interactions between each swash system component (Figure 2) makes it essential that each is properly calibrated and validated within any model. A perennial problem with swash zone model validation has been the paucity of data available with the temporal and spatial resolution necessary to allow proper measurement of the phenomena occurring within the swash. This is due in no small part to the physical and logistical difficulties associated with measurement in the swash zone, both in the field and laboratory. Many swash phenomena occur over very short time scales, and are of small size relative to the measurement precision of the sensors commonly employed. Table 1 summarises the issues surrounding collection of validatory data for some of the main system parameters. Of particular interest for this research are the detailed shape of the swash lens during the uprush, flow reversal and backwash phases as well as the beach surface morphology at the swash event scale.

This paper presents an overview of video measurement techniques and describes experiments undertaken to utilise latest digital video technologies to measure swash water surfaces in a laboratory flume. A review of previously used methods is outlined summarising the history of video measurement in the swash zone followed by a description of the experiments undertaken to compare video data collected using the new techniques with data collected by conventional vertical capacitance probes. Results are summarised and a discussion presented on the issues surrounding the use of new video technologies for swash zone measurement. Conclusions and suggestions are outlined for further experimentation and research.

METHODS

Video measurement of the swash zone

Over the past decade, video recording has become an accepted method of capturing visual records of swash zone and nearshore dynamics in both field and laboratory environments. In many cases, techniques developed for other metrology applications have been adopted for use in the nearshore. These include close range photogrammetric techniques developed for machine vision, medical scanning, industrial and architectural applications as well as airborne and spaceborne remote sensing and image processing. Video has a number of potential advantages over other measurement systems, most notably minimal interaction with the water or beach surface, fast image acquisition rates, relatively inexpensive equipment and minimal logistical requirements. As two-dimensional images, video data are also capable of incorporation within image processing systems, allowing techniques derived for other remote sensing applications to be used to extract relevant hydrodynamic and morphodynamic information.

Notable video applications in the swash zone over the past decade include the 'timestack' method of shoreline position mapping devised by AAGARD and HOLM (1989), which was also used by HOLLAND *et al*., (1995) and HOLLAND and PULEO (2001). In this technique, image processing of the video record at a specific cross-shore position allows the trajectory of the 'shoreline', assumed to be the high contrast foam edge of the swash, to be recorded for each image frame. This technique has since been adopted by the US Army Coastal Engineering Research Center as a method for producing run-up measurements on coastal defences (HATHAWAY and BOTTIN, 1997). HUGHES (1992) used a video camera to record the motion of a bore before collapse to determine initial runup velocity. Photogrammetric techniques have also been used to produce a three-dimensional digital terrain model of the beach face, again from shoreline foam edge measurements (HOLLAND and HOLMAN, 1997). The Argus video system has also utilised a network of video cameras to measure beach and foreshore morphodynamics (e.g. HOLMAN *et al*., 1993; HOLLAND and PULEO, 2001).

Video data have also been used extensively in laboratory swash experiments. LARSON and SUNAMURA (1982) used video images focussed through a transparent flume

Table 1. Swash zone processes and parameters and their measurement.

Sub-system	Phenomenon	Phenomenon description	Measurement characteristics	Measurement systems	Comments
Swash	Uprush / backwash flow velocity.	Water flows in the swash commonly follow an oscillatory, positive landward, negative seaward flow with rapid acceleration and deceleration occurring.	Velocity ranges: 0 m^{s-1} to approximately 5 m^{s-1}. Oscillation from maximum onshore to maximum offshore	Electro-magnetic current meter (EMCM), Acoustic Doppler Velocimeter (ADV), ducted impeller current meters.	Shallow depths cause poor signal to noise ratio or no data, oscillatory flows cause lag for sensors.
	Shoreline.	The time-varying position of the intersection between land and sea, which in the NLSW theory identifies the landward limit of the swash lens during uprush and backwash. Also defines the swash period.	Swash lens depth becomes zero at the shoreline – shoreline velocities will accelerate / decelerate and alternate onshore and offshore	Horizontal resistance wires, or vertical probes, video time stack.	'Shoreline'position can become indistinct in the later stages of the backwash. Poor spatial resolution of the shoreline from electronic probes. Video time stack method relies on foam edge to allow identification.
	Flow reversal.	The middle phase of many swash events, where the shoreline continues to move landwards (i.e. uprush) but the water mass behind the shoreline in the swash lens begins, at least in some places, to move seawards, causing a thinning of the swash lens and potential flow changes.	Same as for swash depth.	Vertical probes, video.	Flow reversal can be short-lived (e.g. less than 3 s). Detailed changes in lens shape may not be identified using probes.
	Time-varying uprush / backwash depth.	Backwash depth can vary over very small cross-shore distances and time scales e.g. due to hydraulic jumps or bores and therefore can act as a determinant of flow velocity. Depth variations also characterise each of the swash phases, uprush, flow reversal and backwash.	Common depths < 0.05m.	Pressure transducers, vertical capacitance, resistance, conductivity probes.	Lagrangian phenomenon – backwash and uprush depths vary over time and space – not well resolved using fixed instruments.
Beach groundwater	Water table elevation	Equilibrium surface at which pore water pressure is equal to atmospheric pressure.		Water table elevation measured with wells which are perforated for their entire length, either manually or	Beach water table elevation depends on tidal elevation, wave run-up, rainfall, and characteristics of the beach

				with pressure transducers. Pore water pressures in the beach measured with piezometers.	sediment that determine hydraulic conductivity, such as sediment size, shape, sorting, and porosity.
	Exfiltration rate	A net outflow of water from the beach matrix into the swash lens subsystem as determined by the hydraulic conductivity and local hydraulic gradient.	Flow rate	Pore water pressures measured at positions in the beach..	Pressures measured rather than rate. Difficult to measure in situ, especially the response to swash.
	Infiltration rate	The net inflow of water from the beach matrix from the swash lens subsystem as determined by the hydraulic conductivity and local hydraulic gradient.	Flow rate	Pore water pressures measured at positions in the beach.	Pressures measured rather than rate. Difficult to measure in situ, especially the response to swash.
	Water table intersection (exit point)	The position where the water table intersects the beach face; determines position of the seepage face and affects infiltration/ exfiltration.	Seepage face develops where the water table coincides with the beachface; distinguished by a glassy surface.	Usually identified by visual observation of glassy surface.	Difficult to identify precise location of intersection. Varies over time
Sediment transport	Transport mode	Dominant transport mode can be sheet flow / bedload or suspended, determined by depth of swash lens, flow velocity, swash asymmetry and other factors such as turbulence length scales.		Traps, optical backscatter sensor, acoustic backscatter sensor	Suspended load measured via traps, OBS or ABS. If sheet flow, traps or fibre-optic OBS only. Difficult to measure the depth of sheet flow.
	Net transport rate	Net transport rate and direction		Traps, profiling	High resolution changes difficult to measure using traditional survey techniques.
Beach face morphology	1st order slope	The average (planar) slope between two points along the beach face – used as a definitive slope value for NLSW swash models.		Profile surveys	Not always representative of the beach topography affecting swash. Temporal variation.
	2nd order slope	Slope variation between two points along the beach face – gives an indication of the geometric nature of the beach face when not planar.		Profile surveys	As for 1st order slope

	Bedforms	Flow-generated bedforms – can influence the flow character of the swash lens and are themselves controlled by flow character.		Micro-profile surveys	High temporal and spatial resolution not easily recorded using traditional survey techniques.
	Roughness	Frictional retardation of the flow determined largely by the size and shape of the sediment making up the beach surface.		Representative friction factor based on sediment size – determined through sediment analysis.	
Sediment	Friction factor	As for roughness.		As for roughness	
	Hydraulic conductivity (K)	Ability of beach matrix to permit water to pass through it , which determines the amount of water lost to the beach on a particular swash event.	Sand: K ≈ 0.01 – 1 cm s^{s-1} Gravel: K ≈ 1 – 10 cm s^{s-1}	Field: piezometer slug tests; laboratory: permeameters	Rarely measured in situ; varies over up to 13 orders of magnitude; spatially variable across beach.
	Permeability (k)	Measure of the ability of sediment to transmit fluids.	Sand and gravel 10^{-3} to 10^{-8} cm^2	Field: well tests; laboratory: permeameters	Intrinsic or specific permeability; difficult to measure in situ.
	Moisture content	Volume of water in sediment sample divided by the total volume of the sediment; affects hydraulic gradient, infiltration/ exfiltration.		Time domain reflectrometry, ThetaProbe, neutron probe	Cannot be measured at high frequencies.
	Size	Representative sediment size controls hydraulic conductivity and the friction factor.		Sediment size analysis – sampling and size distribution	Difficult to measure in situ; high degree of variability.
	Fall velocity	Determined by the size and density of sediments. Fall velocity will help determine the transport mode.		Sediment size analysis	Difficult to measure in situ.

wall to qualitatively identify swash processes through the flow characteristics. PETTI and LONGO (2001) also collected two-dimensional images of the swash lens, apparently using an edge detection algorithm to highlight water surface edges, to provide qualitative estimates of turbulence during the breaking process. MATSUNAGAand HONJI (1980) used a similar technique, with cine cameras, to measure flow velocities within the swash via neutrally buoyant particles.

FOOTE and HORN (1999) used a two-dimensional technique similar to that used by LARSON and SUNAMURA (1982) to image the detailed cross-shore swash lens geometry in a laboratory flume, with the aim of extracting metric data from them. The images were imported into a geographical information system (GIS), the water surface edge digitised from each video frame and a comparison with measurements made from conventional vertical probes was attempted. This suggested that video measurement of swash could be used as a comparable technique for the measurement of water surfaces in the laboratory, although it was recognised that further comparisons had to be made to fully determine the applicability of the technique to laboratory measurements. The FOOTE and HORN (1999) experiments used interleaved scanning CCD camcorders, recording on Hi-8 analogue tape to capture the images. A-D conversion was performed using a VITEC ISA RT5 MPEG encoder / decoder card. The resulting MPEG-1 movie file was converted into single frame JPEG images using a shareware converter, HYMPEG. Difficulties with the conversion process as well as the issues surrounding interleaved data capture and subsequent digitisation made the use of the data collected during the 1999 experiments for measurement of swash events problematic.

Like many electronic recording systems, video technology has undergone significant development over the past decade, with the result that new systems and recording media have become increasingly available for measurement data collection. Of particular interest has been the advent of digital video imaging and recording which provides the capability for real time digitisation of images and storage direct to PC via IEEE1394 transfer standards.

In all video measurement applications, there are a number of steps which must be undertaken (Figure 3).

- video sensing
- video storage
- frame-by-frame export
- image analysis and measurement

The main issues surrounding the use of video as a primary measurement tool are related to these steps. Each step requires a series of processes to be undertaken, and each of these processes can introduce bias or error into the values collected.

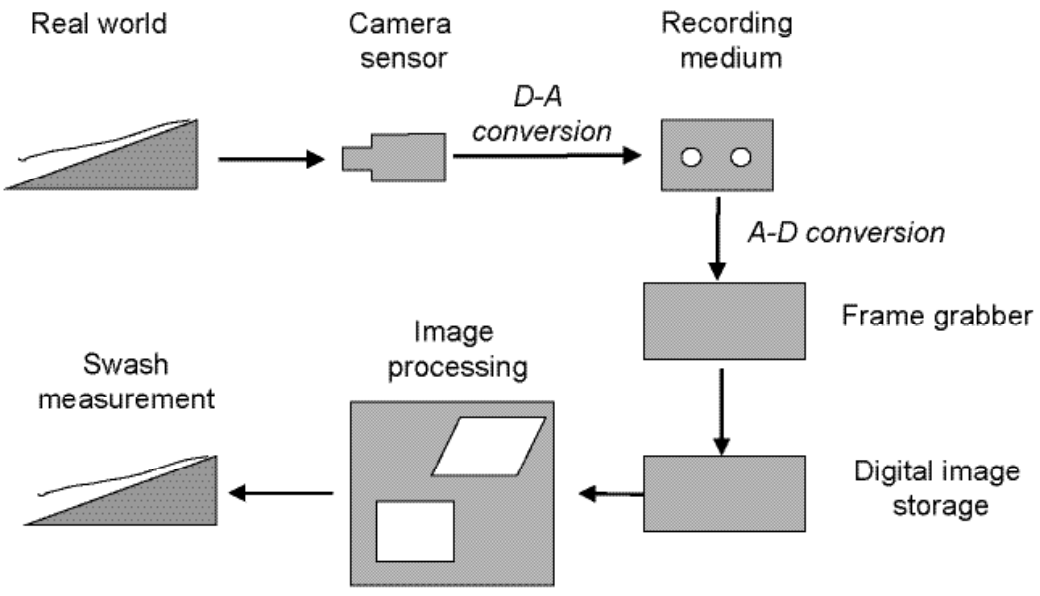

Figure 3. Video imaging and measurement process (after CLARKE *et al*., 1995)). This schematic illustrates an analogue system. Digital (IEEE1394) systems remove the D-Aanalogue recording and frame grabber stages from the post-processing environment.

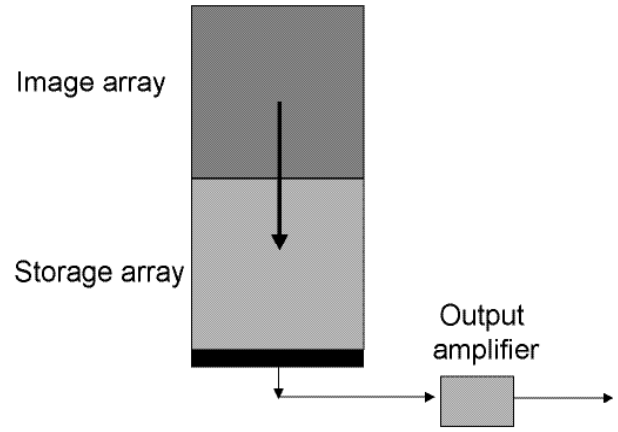

Figure 4. Frame transfer CCD process. The active pixels of the imaging array shift their charge to the relevant cell in the storage array. These are then moved to the storage system via an amplifier while the next set of charges are collected by the image array.

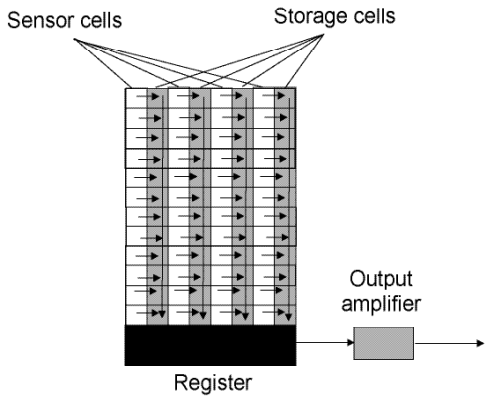

Figure 5. Interline transfer CCD process. The active pixels of each imaging cell column transfers their charge to the adjacent storage cell. Each sensor cell charge is then shifted down to the register while the next charge is collected.

Video capture

There are a number of video capture systems available. The range of technologies and standards used vary both by country and by intended application. The choice of video system for swash measurement applications is therefore important as the resulting accuracy is determined in a large part by the initial system parameters.

Charge Coupled Device sensors

Many of the applications described above have made use of commercially available camcorders, or in some cases discrete video camera heads, as the imaging system. The imaging sensors of most camcorders and cameras are based on the Charge Coupled Device (CCD) method. A CCD is a two-dimensional array of photoelectric sensors, each of which generates a charge when struck by photons from the electromagnetic radiation (EMR) arriving at the sensor surface focussed through a lens. The charge is collected, amplified and stored as a voltage. Timing signals are added to the start and end of each block of pixel charges to aid reproduction of the full image in the display system. In this way, the CCD array acts in the same way as the film in a standard camera, positioned at the focal plane of the camera. The charge from each CCD cell is collected and stored as a discrete, digital number (Dn) value. CCDs transfer the charge from each photoelectric cell by one of two transfer modes, interline or frame (CLARKE *et al*., 1995). Frame transfer CCDs include a secondary array of pixels which are used to temporarily store the charge from each cell in the ‘active’array, whilst the next charge is being collected (Figure 4).

Interline CCDs are constructed to allow each active column of pixels to be separated by a row of storage pixels. This allows the charge from each active pixel to be transferred across to the adjacent storage cell before shifting down to the serial register at the base of the CCD chip (Figure 5). The advantage of the interline method is the short time period required to transfer the charge across to the storage cells, which reduces the potential for image bias or jitter from moving objects, as well as increasing the camera frame rate and hence temporal resolution.

Interleaved vs progressive scan

Most previous video applications in the swash have also utilised the traditional ‘interleaving’ scanning system. This is a throwback to the early television ‘half-frame’ system, where a complete television image is created from two ‘fields’, scanned at twice the rate of the full frame, one containing data for the ‘odd’ rows, the other data for the ‘even’rows. In interleaved video images, pixel voltages are stored in the same ‘odd/even’ order. This can also increase image error through the reduction of true vertical resolution (Figure 6).

Progressive scan cameras scan each row in order and store the complete, full frame, image in one go (Figure 7). As a result, fast moving objects are not recorded over two separate time periods and then merged as with interleaved images. Instead, images are constructed from one scan exposure period. This reduces the amount of time correction required to reproduce each image and also minimises image jitter. Progressive scan is a relatively new technology and is

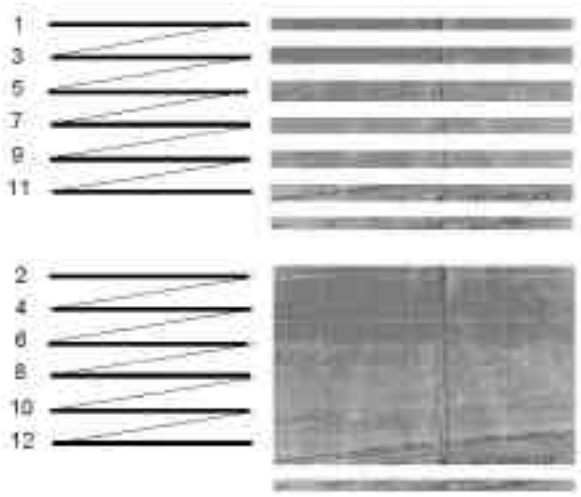

Figure 6. Interlaced scanning. Field 1 scans 'odd'lines of pixels and stores to the register. Field 2, a half frame cycle later, scans the 'even'fields and adds those to the full frame image. The complete image is therefore constructed from two scans, each taking a half frame cycle to be collected.

not available on most off-the-shelf camcorders. However, the availability of progressive scan cameras in the higher end products is becoming more widespread, particularly in the fields of industrial and medical metrology. It is clear that the exposure time of each scan is critical, when imaging moving objects such as swash, in determining the amount of motion skew within each full image. Even though the maximum frame rate is controlled by other factors (particularly the data shift and storage rate) it is important that the exposure time is controlled to reduce the amount of motion error encountered, whilst allowing an acceptable quanta of electromagnetic energy to be collected by the CCD. High-speed video cameras allow both exposure time (via the shutter speed) and frame rate (via the data storage) to be much higher than standard. However, such imaging systems are not readily available and it could be suggested that for the purpose of imaging swash phenomena, a 15 frames per second frame rate, with an optimal exposure time, is ample for the collection of data.

Spatial, radiometric resolution and colour imaging

Spatial resolution can nominally be defined as the imaging size of each picture element (pixel) which makes up the full image frame. A more accurate description of the spatial resolution is the instantaneous field of view (IFOV) which describes the minimum resolvable object. The number of cells in the CCD array defines the nominal sampling area of each pixel. In most CCDs, however, the number of 'effective' pixels is lower than the total number

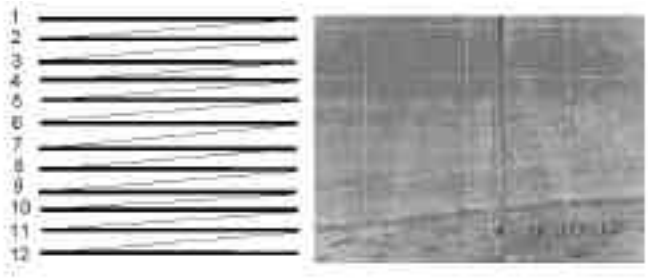

Figure 7. Progressive scanning. Odd and even rows are scanned in the full order and a single full frame image stored.

of pixels in the array. Also, the number of output pixels (those used to create the final image) is lower than the number of effective pixels. As such, the IFOV is determined in part by the total image field of view (FOV) as measured by the 'real world' horizontal distance of the image plane, divided by the number of pixels in the output image.

Of particular importance in determining the IFOV is the amount of 'contrast' between objects as recorded by the sensor. Greater contrast allows for better spatial resolution. As all natural objects, including water, reflect EMR at varying levels of efficiency over different wavelengths, increased contrast can be achieved by sampling the radiation in different sectors ('bands') of the electromagnetic spectrum (EMS). CCDs are commonly sensitive to EMR in the visible and very near infrared (VNIR) bands (wavelengths between 400nm and 700nm). In most cases, CCDs record three 'bands'of data (Figure 8), relating to the blue (400nm to 500nm), green (400nm to 600nm) and red (600nm to 700nm) wavelengths. The VNIR

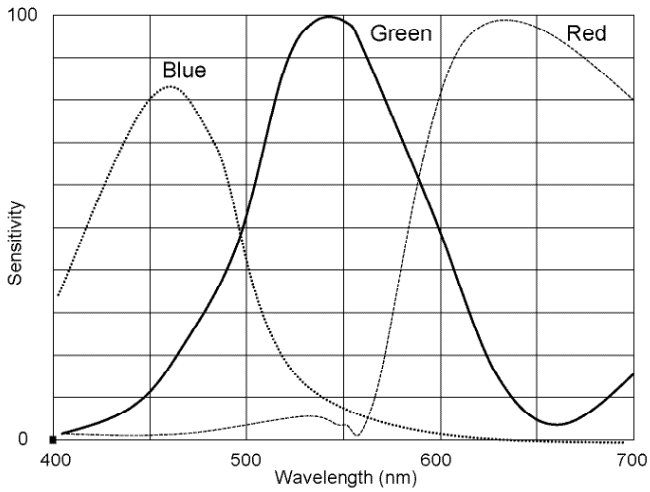

Figure 8. Approximate CCD spectral sensitivities. After Sony (2000)

sensitivity (seen in Figure 8 as a tail-off of the response towards 700nm) is often filtered out, either by recourse to optical filters or by coatings on the sensors. Early video systems used a series of 'colour wheel' optical filters to limit EMR reaching each CCD cell to a particular wavelength in turn (KODAK, 2000).

Newer systems provide three separate cells, each coated to be sensitive to each of the three bands (KODAK, 2000; WATKINSON, 1994). By combining the red, green and blue bands (RGB), a full range of visible light colours can be recreated in display devices and image processing systems. The transmission and storage of three colour bands is, however, data expensive, and in order to minimise the required data storage or transmission bandwidth, colour difference values are created during the imaging process.

Video storage

Analogue video recording systems such as Hi-8 or VHS have been used to store the resulting images on tape for later off-line processing. Such systems require significant analogue to digital (A-D) conversion to allow eventual image processing and data extraction (see for example, FOOTE and HORN, 1999). At each stage, image (and therefore measurement) degradation may be introduced.

The storage of video data once captured also provides a number of options. Most off-the-shelf camcorders record the full image data either as analogue or digital signals, stored on a re-recordable tape. VHS and S-VHS tape formats have been used to record video of swash in the past (e.g. AAGAARD and HOLM, 1989; HOLLAND *et al.*, 1995). VHS provides the greatest data bandwidth of all video formats. Hi-8, which is more compact than other formats, provides the best image quality. Recently, MiniDV has been used to record data in digital format for later frame grabbing. The use of intermediate recording media can be an advantage when collecting large amounts of data in the field, as it provides a relatively inexpensive archiving format. However, the addition of further conversion stages at recording and during PC data import can result in increased data degradation, especially as the result of line jitter from synchronisation errors during recording and playback and image noise due to tape imperfections and mechanical discrepancies (SHORTIS *et al*., 1993).

Digital direct data transfer

Direct transfer of images to PC disk as performed here is possible using the IEEE1394 high bandwidth data transfer serial bus. This provides a data transfer standard which allows data transfer at rates of up to 400 Megabits per second. As such, it provides a means of allowing high frame rate data download of image data such as that from 3-colour high resolution digital cameras at up to 15 frames per second, in isochronous (real time) mode. A potential increase in the temporal, spatial and radiometric resolution of the images captured through increased quality sensors and a reduction of error in the data conversion process is therefore possible using progressive scan and digital data transfer, rather than standard analogue camcorder technology.

EXPERIMENTAL DESIGN

The objective of the experiments described in this paper was to test the applicability of digital video technology in the production of images of the swash lens in a laboratory environment. It was hoped that digital video would provide an improved spatial and temporal resolution, increasing the contrast between water and background pixels to aid in the automatic / semi-automatic edge detection process or increase the accuracy of manual digitisation.

A Sony DFX-X700 interline transfer progressive scan digital camera was used to capture the swash images. The camera operates at frame rates of either 7.5 or 15 frames per second, and stores images in the YUV (4:2:2) colour data format. Table 2 provides key functional parameters for the DFW-X700 camera. A J6 x 11 MACRO C-mount lens was used to allow manual focussing.

Table 2. Key functional parameters of the DFW-X700 camera (SONY, 2000).

Image sensor	1 / 2 -type progressive scan CCD
Effective pixels	Approximately 800,000 (1034 H x 779 V)
Output pixels	1024 V x 768 H
Interface format	IEEE1394-1995
Protocol version 1.30	1394-based digital camera specification
Data format (used)	1024 x 768 YUV(4:2:2)
Frame rate	7.5 fps or 15 fps
Transfer speed	400 M bps
Lens mount	C- mount
Minimum illumination	20 1x (F1.4, gain + 18dB)
Shutter	2s to 1/20000s
Gain	0 to 18 dB

An Armfield open channel tilting flume, 7 m in length, with transparent sides, 0.3m width, 0.45m depth, was used to run a series of monochromatic waves, period = 2.5 s, wave height = 0.06m, in a water depth of 0.18m against an impermeable planar beach, with a slope of tan = 0.252 (Figure 9). These parameters were chosen to provide a swash event on the beach with clearly defined uprush and backwash phases. Control markers were added to the flume side at 0.1m intervals, to allow proper metric calibration of the images during post-processing. Design of the control

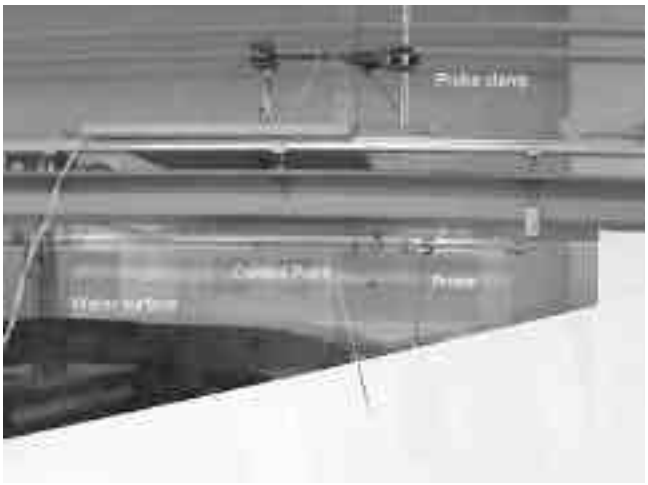

Figure 9. Image of the flume showing the wave gauge rig, beach face and control markers.

markers followed a recommended method for photogrammetric image control (CLARKE, 1994). Paper was pasted to the flume wall to increase background opacity. The water was dyed using potassium permanganate in order to maximise image contrast.

A single standard surface piercing resistance type wave gauge was used to record analogue water depth signals. Wave gauge data were recorded as ASCII time/voltage pairs on a laptop computer via an A-D board, logging at 10 Hz. The absolute accuracy of the vertical wave gauge is of the order of ±1 mm; however, the bottom 10mm of the wave gauge was encased in plastic resin and was therefore not collecting data. As a result, no data were recorded within 10mm of the bed.

A series of 2.5 minute runs were made, recording the swash event simultaneously with the wave gauge and video systems. Water surfaces were measured with the wave gauge at an x-axis position 66.7cm 'landward' of the arbitrary datum. This was in order to get measurements in the beginning phase of the uprush, where velocities and depths were expected to be greatest, therefore providing the worst possible motion error. A 1 minute long data set has been used in this analysis from the first run.

Synchronisation of wave gauge and video

In this experiment, digital time synchronisation between the camera and wave gauge data through an external trigger was not used. TTL, or 'time to live' uses a pulse signal generated by the host PC which 'holds'data such as images and ASCII string data such as that collected from a wave gauge, for a specified time period, assigning a defined name to them. In this way, video and other data can be synchronised within the same application. The computer system available for the experiments reported here did not allow the use of TTL; instead, the data recorded on the wave gauge was matched to that from the cameras by visually identifying the peak of the first swash event on the wave gauge data.

Data capture

The following system specification was used to capture the swash images. The DFW X700 camera was connected via a 1.5m IEEE1394 specification cable to a Unibrain Fireboard 400 IEEE1394 compatible PCI host adaptor card. This was connected via an expansion port to a Dell Precision 420 Pentium III dual 800 Mhz processor PC, running NT version 4, service pack 6. 20 Gigabytes of hard disk were available for data storage. A read-write CD-ROM port was also available for data transfer to CD-ROM.

The Unibrain ubCore IEEE1394 drivers were used to provide the low-level control of the PCI card and connected camera. Unlike standard camcorders, digital cameras are controlled via commands to the control and status register (CSR). The Fire-I interface version 2.0 (beta) was used to define the settings and controls required to create image data from the camera.

Camera settings as used for data capture

Table 3 lists the settings for the main CSR options used for this experiment. As can be seen, the shutter speed was changed to 17.01 milliseconds in order to reduce object motion error. As a result, the gain setting was also changed to 14.7dB to allow for increased image contrast. Image collection rate was set at 133 ms, thus approximating to the 7.5fps camera frame rate.

Video data collection

The digital camera was positioned 91cm from the flume side. An artificial planar, impermeable beach face was inserted to allow run-up to be generated. Six control points were attached to the flume (Figure 10). These were used to provide metric calibration of the images during post-processing and off-line measurement.

The data collected by the Fire-I software was stored as individual RGB SVGAcompatible images, each 1.37Mb in size. A 2.5 minute run resulted in 1.06Gb of images. These were compressed to approximately 300Mb.

RESULTS

Comparison of swash depths measured with wave gauge and video

Measurements from the video data were collected through manual digitisation of the water surface at the wave gauge position using a geographic information system (GIS),

Table 3. Video settings used in the experiments.

Video Format	SVGA / VGAnon-compressed
Video mode	800 x 600 pixels
Speed	200 Mbps
Frame rate	7.5 fps
Hue	164 (range 83 – 173)
Saturation	95 (range 0 – 255)
U/B	173 (range 0 – 255)
V/R	137 (range 0 – 255)
Exposure	136
Shutter	17.01 ms (range 2006ms – 50µs)
Gain	14.7 dB (range 0 – 18)
Brightness	96 (range 96 – 233)
Sharpness	3 (range 0 - 7)
Gamma	129 (range 128 – 130)

ArcView 3.1. A manual digitisation technique was chosen as automatic edge detection did not produce accurate water surface edges for all images due to image noise and the effects of perspective creating duplicate edges in some cases. A manual interpretation of the water surface against the surrounding image noise was relatively easy in the majority of images due to the potassium permanganate within the water. The use of the ArcView software allowed for increased interpretation to be made for each image by allowing the user to zoom in and out of the image. This increased the accuracy of the digitisation process. An accuracy check was done by digitising points from the same images twice and comparing the results (Figure 11). This showed that the range of variations between 106 point comparisons was +2.3mm to –1.1mm with a mean difference of 0.2mm. Only two or three outliers accounted for the larger values. The majority of the differences were due to difficulties in identifying the lowest depths (below 1mm) of the backwash phases. Most of these differences could be considered to be within the resolution of the imagery, suggesting that the manual method could provide consistent data quality.

By identifying the position of the water surface intersection against the wave gauge line, it would be possible to determine the water depth for that image. This was deemed a valid method as the images were relatively high resolution. Images were not geo-rectified as they were seen to be relatively planar. Depths could be collected along a single vertical line, defining the position of the wave gauge in the image. Each image was opened in its original BMP format within a map 'view'. Image co-ordinates were converted to calibrated metric values by creating a vertical line file between two control points (see Figure 12) which was then overlaid onto the image files at the position of the wave gauge / beach intersection. The metric distance for this line was recorded within the application as was the start and end positions of the file in 'map' co-ordinates. From this information, the relative distance along the line could be determined for each digitised water surface position as a percentage of the line distance and then converted into metric depth values.

A customised tool was developed using ArcView's object-oriented development language, Avenue. A control panel allowed the user to define an output ASCII text file for the digitised depth values to be stored in. A list of loaded image files was also added. As each image was selected from the list, the image was displayed on the screen. The user then clicked on the screen at the intersection between the water surface and the wave gauge line. The Unibrain software names the image as it is collected with the date and time (to the millisecond). This was collected and stored with the calculated depth value. This allowed the data to be plotted in a spreadsheets as time and depth values in the same way as the wave gauge data. 70 seconds of water surface points were captured in less than 2 minutes using the manual digitisation interface.

A comparison of the wave gauge data and the video data for approximately 1 minute of data can be seen in Figure 13. The wave gauge was positioned at the still water level

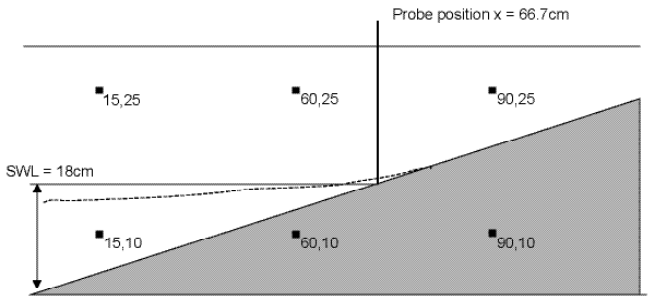

Figure 10. Diagram of control markers and beach geometry in the flume during imaging. All co-ordinates are measured in centimetres from an arbitrary datum.

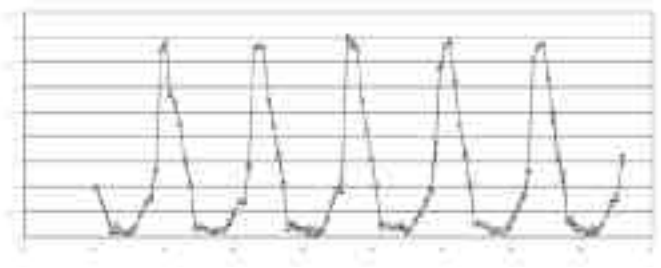

Figure 11. Comparison of two separately digitised swash records for the same images. Time(s) is plotted along the x axis. Depth (cm) is plotted along the y-axis. The open squares are run 1 and the closed squares are run 2.

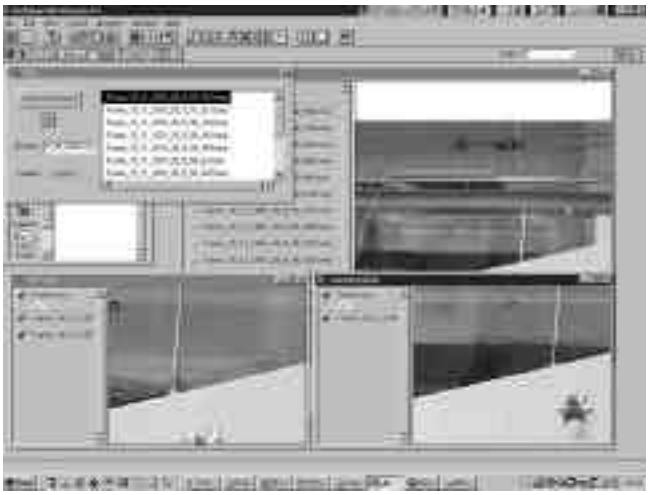

Figure 12. Screenshot of the customised ArcView interface which allows for manual digitisation of the water surface at a pre-defined location. The white line is the wave gauge position. This line is of a known length. All digitised depths are calibrated from this length. Festive ornament for scale.

shoreline position. The lack of an instantaneous synchronisation signal meant that the data could not be easily compared. The truncation of the wave gauge data in the lowest flows due to the plastic base made it impossible to identify the point of swash uprush in each record. Instead, the two data sets were joined by identifying the first maximum swash depth in both records. The differences in the video and wave gauge sampling periods also made a point-to-point comparison difficult. However, a general comparison shows that there is a good general correlation between the wave gauge and video data. A comparison of the 30 measured maximum wave gauge values for both records showed that the mean values differed by 0.15mm.

The video data also identified some small systematic secondary peaks in the water surface, particularly in the first part of the uprush phase. Again, the truncated wave gauge data set did not allow these harmonics to be identified in the wave gauge data set and it is therefore impossible to confirm their actual existence.

Image processing and automatic edge detection

ERDAS Imagine provides image processing functions such as edge detectors to enhance imagery and extract information held within them. The ERDAS Sobel edge detector was used to identify zones of high spectral contrast in the image, such as between the water surface and its background. As can be seen in figure 14, the Sobel edge detector, based on two 3x3 matrices, recalculates each image pixel to denote the gradient of spectral difference

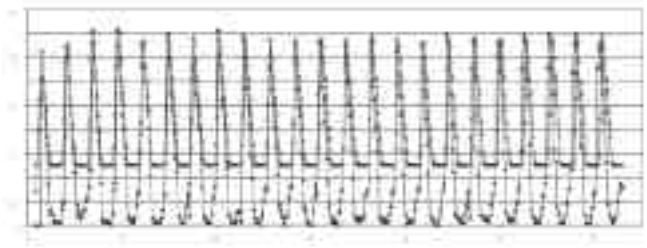

Figure 13. Comparison of water depth measured with the wave gauge and the video. The open squares are the depths measured with the wave gauge and the closed squares are the depths measured with the video.

between the central pixel and its surrounding 8 pixels (ERDAS, 2000). The Sobel detector is non-directional; the matrices do not favour contrast gradients in any particular direction. The result is an image with greater intensity values along ‘edges’ and lower intensities where adjacent pixels have relatively homogenous spectral values. The water surface edge is visible in the majority of the swash lens as a bright line. There are a number of other edges visible, which are the result of other areas of high spectral contrast.

It was not possible to produce vector lines directly from the ERDAS software for the edge detected images. However, a manual digitisation of the water surface edge from a complete swash event can be seen in figure 15. It was possible to digitise (in ArcView) the complete surface, including the turbulent bore face where the edge was less pronounced. The resulting surfaces can then be overlaid to identify changes in swash geometry for each frame. It is clear from figure 15 that the use of digitised edges can produce high-resolution instantaneous measurements of water surface depth across the whole water surface rather than at a single location such as from a wave gauge.

DISCUSSION

The comparison of the wave gauge data and the video measurements has provided some indication that the video data are comparable to that being collected by the wave gauge. In general terms and through analysis of the peak swash elevations at the wave gauge position, it appears that there is a close correspondence between the two measurements. The insensitivity of the wave gauge due to the plastic endpiece resulted in the lack of data in the lower backwash and uprush phases. However measurement of very shallow swash depths is a problem with any current measurement system. No comparison can therefore be made from these data of the video data’s measurement accuracy

Figure 14. Example non-directional edge detection (Sobel). Control markers can be identified as can the main water surface edge. Note the lack of definition at the turbulent edge and the duplicate edge from the perspective effect, although it is still possible to make out the edge by eye along most of the swash length.

during the time of small swash depth. Figure 11, which plots two manually digitised swash records, indicates that overall there is consistent digitisation accuracy with the greatest differences occurring in the lowest depths. Most differences are within 1mm to 1.5mm. This is close to the minimum resolvable unit of the images. The truncation of the wave gauge record also resulted in the need for a shifting of the wave gauge data to take account of the vertical difference in height at that point. This shifting does not account for the lack of data in the lowest 12.5mm as the plastic block measured 10mm in the vertical. The other 2.5mm may be the result of wave gauge resolution or may reflect inaccurate synchronisation between the wave gauge and video data sets.

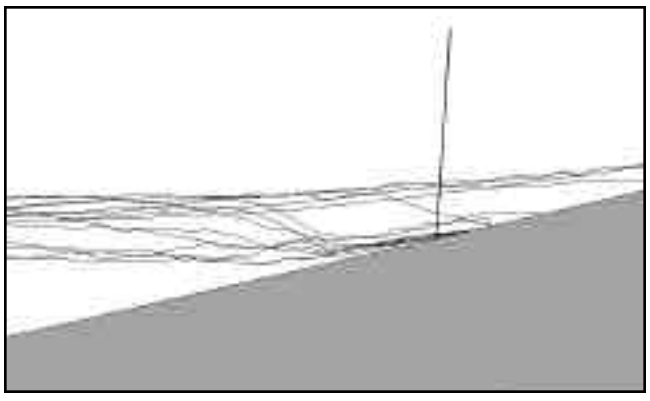

Figure 15. Example of manually digitised water surfaces from images after Sobel non-directional edge detection. The near-vertical line denotes the wave gauge position. Note the high-resolution undulations in the shallower water surfaces

There appears to be some evidence of a difference in the apparent swash period between the two systems (see the last 5 or 6 swash events in Figure 13). There may be some small difference in the exact time of the peak in each record due to the difference in the sampling frequencies. The lack of an exact synchronisation between the data sets makes exact comparisons difficult and the use of a TTL pulse trigger mechanism would ensure correct synchronisation. However, in this case the technological limitations of the wave gauge and its logging system made the use of TTL impossible.

The use of digital video recording removes the need for analogue to digital conversion of imagery. As individual image files, each ‘frame’ of data can easily be incorporated into spatial analysis software such as GIS or image processing. This is a distinct logistical advantage, reducing the amount of time required for data conversion and preparation as well as the number of data modification stages. The use of ‘real time’ data collection to PC also makes the use of on-line processing systems possible, for instance to store water surface geometry for each image in near real time. This is however, reliant on the ability of the data to be automatically processed and for the extraction of accurate water surfaces to be made. Visual inspection of the images indicates that the spatial and spectral consistency of the digital data is also greater than that produced using analogue systems. However, there is still difficulty in identifying the true water surface without the use of manual interpretation. While it is possible to generate consistent measurements from manual digitisation of the water surface, the use of automatic methods would enable faster processing and hence increased data collection. The use of a non-directional edge detector such as the Sobel algorithm provides a means of identifying all areas of the image where there is a significant change in the spectral ‘texture’ of the

image through a convolution matrix. However, the identification of a single linear edge such as that of the water surface compared to the background detail relies on the ability to isolate the pixel signatures of the water body. This is not easy when there are numerous other features being imaged in the frame, such as the wave gauge, the flume and specifically in the case of the images collected here, the perspective effect of the far side of the flume. Possible actions to reduce the effects of such 'noise' are to re-position the camera to reduce the impact of the perspective effect as well as increase the contrast between the water body and its surroundings through increased opacity. The potential for infrared imaging as a means of increasing water body opacity and hence image contrast has not been investigated in this research. CCD sensors are available which are sensitive to the near infrared. These could be used to enhance opacity as water tends to produce very low reflections in the infra-red wavelengths (LILLESAND and KIEFER, 1987).

Another limitation to real time measurement is the need (when digitising across the whole of the image) for geo-rectification to be undertaken to convert from image co-ordinates to cartesian co-ordinates. This can be done relatively easily using image processing systems such as ERDAS Imagine. Polynomial transformations can be employed to warp the images based on the control points available in the image. However, this process relies on the manual input of the control points, at least for the first image. Automated rectification can be undertaken for subsequent images provided there is no change to the image extents or scale between images. This is easier to control in the laboratory than the field. All geometric correction procedures treat the image pixels as positions within a two-dimensional array. The convolution process then resamples each cell and populates a new 'planimetrically correct' image array by estimating the pixel brightness (digital number) based on the particular resampling method employed. In all cases, there is a consequent loss of data or change in the geometric orientation of the pixels in relation to each other, as well as the potential for changes in the radiometric properties of the image (CAMPBELL, 1987; LILLESAND and KIEFER, 1987). The use of a local vector calibration technique, such as that used for the digitisation of water depths at the wave gauge position, removes the need for such correction. This is not practical for measurement across the image, however, as lens and CCD distortions will cause variations in the positional accuracy of the calibration away from the control points used.

It is evident, however, that the video data provide a satisfactory measurement of the swash depth in comparison with the wave gauge data and in the case of the smallest water depths, provided greater detail due to the truncation of the record in the lowest flows. Small differences in the data sets could also be attributed to the observed super-elevation of the swash depth at the wave gauge position due to flow interference. This was seen during the experiment to cause up to a 200% increase in the measured water surface in the wave gauge record. The use of video as a measurement system allows for such spurious measurements to be identified.

It is clear from this work that the quality of the data collected by digital camera is strongly dependent on the specification of the host PC, in particular the available RAM and hard drive speed. It is possible using software such as Fire-I to optimise the image resolution and frame rate to the particular machine specification. However, a number of hardware-related difficulties were encountered during the video collection process, the most notable being the propensity for image duplication and frame timing error to occur if the transfer buffer was exceeded. This was minimised through the reduction of the transfer and frame rates to 200 Mbps and 7.5 fps respectively. The large data sizes collected even when using reduced image quality and transfer rates meant that images could only be collected for relatively short time periods (two to three minutes) before the disk storage sizes became large. This is, however, appropriate for the swash geometry analysis. Basic PC management techniques, such as the disabling of virus checking software, the shutting down of other programs and the optimisation of the disk management procedures can also help to optimise data collection. Image file compression can reduce storage to a tenth or less of the original disk space. It is possible to argue that the advantages of consistently high spatial resolution, as well as the immediate availability of the images for digital processing outweigh the limitations described here.

The Sony DFW–X700 camera also provides a number of functions which could be employed to enhance the data capture process. For instance, the image size and extent (and hence the data transfer volume) can be reduced through the use of the partial scan function (SONY, 2000). This allows the user to define a subset area of the image in 1/8th minimum units via the CSR commands. The Fire-I software does not currently provide this function as a standard tool, although it is possible using the customisable Unibrain software to produce reduced size images.

CONCLUSION

Experiments to evaluate the applicability of digital video to the capture of image data for the measurement of time-varying swash geometry have been undertaken in laboratory conditions. A Sony DFW-X700 digital video camera was used to record, direct to PC hard drive, standard SVGA RGB images at a predefined frame rate, from which swash depths were extracted through the use of GIS and image processing techniques. IEEE1394 data transfer technology was employed with the assumption that the removal of

analogue-to-digital conversion stages and half-frame interleaving as used in conventional analogue video would result in higher-quality image data. In comparison to analogue video, digital video reduces the number of processing steps required to extract swash geometry measurements. The main differences are due to the real time nature of the recording medium direct to PC. This reduces the need to convert from analogue to digital and therefore reduces the potential for image degradation. The use of digital technology also reduces the potential of error due to tape distortion and the problems of half-frame interlacing. As a result images are of higher geometric quality than equivalent analogue data. The following conclusions can be made:

a) Data were collected as digital images using the IEEE1394 transfer at a frame rate of around 7 fps direct to PC hard drive. Manual digitisation of the water surface using a GIS provided high-resolution measurements of the swash lens geometry for each frame. It was also possible to enhance the water surface using a standard edge detection algorithm. However, automatic extraction of the water surface was not possible from these images due to the presence of spurious edges and other noise, particularly as a result of perspective effects from the flume walls. This impact could be reduced by varying the camera angle with respect to the flume wall.

b) A comparison of manually digitised depths to wave gauge data collected at the time of imaging suggest that the data captured by the video system are comparable to that collected by the wave gauge. Problems with wave gauge/video synchronisation made exact comparison difficult. However, an analysis of the time series swash depths indicate that the data collected by the video are applicable to micro-scale swash measurements, including the measurement of surface undulations across the whole swash lens.

c) The large data transfer rates of the images require a PC with at least the specification used here. Changes to the camera status and registry settings can potentially reduce image data sizes, therefore allowing increased transfer rates and better temporal resolution.

ACKNOWLEDGEMENTS

Postgraduate study assistance for MF was provided by the Department of the Environment and Intermediary Systems Limited. We would also like to thank Mr Antonis Papadatos of Unibrain for support with the Fire-I software, Dr Tim McCarthy for loan of the camera and advice on digital video capture, and Dr Stuart Robson of University College London and Professor Mark Shortis of the University of Melbourne for advice with video metrology.

LITERATURE CITED

AAGAARD, T. and HOLM, J., 1989. Digitization of wave run-up using video records. *Journal of Coastal Research*, 5 (3), 547-551.

CAMPBELL, 1987. Introduction to remote sensing. Guilford Press, New York. 551pp.

CLARKE, T.A., 1994. *An analysis of the properties of targets used in digital close range photogrammetric measurement*, SPIE Videometrics III. Boston. 2350 251-262.

CLARKE, T.A., COOPER, M.A.R., CHEN. J. and ROBSON S. 1995. Automatic three dimensional measurement using multiple CCD camera views. *Photogrammetric Record* 15(85), 27-42.

ERDAS, 2000. *Online Field Guide*. ERDAS INC.

FOOTE, M. and HORN, D.P. 1999. Video measurement of swash zone hydrodynamics. *Geomorphology*, 29(1/2), 59-76.

HATHAWAY, K.K. and BOTTIN, R.R. 1997. *Video measurement of wave runup on coastal structures*. Coastal Engineering Technical Note CETN-VI-28 3/97, US Army Corps of Engineers Waterway Experiment Station, Vicksburg, Mississippi.

HOLLAND, K.T., RAUBENHEIMER, B., GUZA, R.T., and HOLMAN, R.A. 1995. Runup kinematics on a natural beach. *Journal of Geophysical Research*, 100(C3), 4985-4993.

HOLLAND, K.T. and HOLMAN, R.A. 1997. Video estimation of foreshore topography using trinocular stereo. *Journal of Coastal Research*, 13 (1), 81-87

HOLLAND, K.T. and PULEO, J.A. 2001. Variable swash motions associated with foreshore profile change. *Journal of Geophysical Research*, 106(C3), 4613-4623.

HOLMAN, R.A., SALLENGER, A.H., LIPPMANN, T.C. and HAINES. J.W. 1993. The application of video image processing to the study of nearshore processes. *Oceanography*, 6(3), 78-85

HUGHES, M.G. 1992. Application of a non-linear shallow water theory to swash following bore collapse on a sandy beach. *Journal of Coastal Research*, 8, 562-578.

HUGHES, M.G. 1995. Friction factors for wave uprush. *Journal of Coastal Research*, 11(4), 1089-1098.

HUGHES, M.G., MASSELINK, G. and BRANDER, R.W. 1997. Flow velocity and sediment transport in the swash zone of a steep beach. *Marine Geology*, 138, 91-103.

HUGHES, M.G., KEENE, J.B. and JOSEPH, R.G. 2000. Hydraulic sorting of heavy mineral grains by swash on a medium-sand beach. *Journal of Sedimentary Research*, 70(5), 994-1004.

KODAK 2000. *Kodak CCD Primer #KCP-001*. Eastman Kodak Company - Microelectronics Technology Division B81, Floor 5, RL, Rochester, NY 14650-2010. 13pp.

LARSON, M. and SUNAMURA, T., 1993. Laboratory experiments on flow characteristics at a beach step. *Journal of Sedimentary Petrology*, 63(3), 495-500.

LI, L., BARRY, D.A., PATTIARATCHI, C.B. and MASSELINK, G. *In press*. BeachWin: modelling groundwater effects on swash sediment transport and beach profile changes. *Environmental Modelling and Software*.

LILLESAND, T.M. and KIEFER, R.W., 1987. *Remote sensing and image interpretation*. 2nd edition. Wiley, London, 721 pp.

MASSELINK, G. and HUGHES, M.G., 1998. Field investigation of sediment transport in the swash zone. *Continental Shelf Research*, 18, 1179-1199.

MASSELINK, G. and LI, L. 2001. The role of swash infiltration in determining the beachface gradient: a numerical study. *Marine Geology*, 176, 139-156.

MATSUNAGA, N. and HONJI, H. 1980. The backwash vortex. *Journal of Fluid Mechanics*, 99(4), 813-815.

PETTI, M. and LONGO, S. 2001. Turbulence experiments in the swash zone. *Coastal Engineering*, 43, 1-24.

PULEO, J.A., BEACH, R.A., HOLMAN, R.A. and ALLEN, J.S. 2000. Swash zone sediment suspension and transport and the importance of bore-generated turbulence. *Journal of Geophysical Research,* 105(C7), 17,021-17,044.

SHORTIS, M.R., SNOW, W.L., CHILDERS, B.A. and GOAD, W.K. 1993. *The influence of storage media on the accuracy and repeatability of photogrammetric measurements using CCD camera*. SPIE Videometrics II, 2067, 80-92.

SONY 2000. *CCD Colour Digital Camera Module DFW-SX900, DFW-X700 Technical Manual (Version 1.0) - English*. Sony Corporation. 47pp.

WATKINSON, J., 1994. *An introduction to digital video*. Focal Press, London, 311pp.